Atmos. Chem. Phys., 15, 3429–3443, 2015
www.atmos-chem-phys.net/15/3429/2015/
doi:10.5194/acp-15-3429-2015

Atmospheric Chemistry and Physics
Open Access

Total sulfate vs. sulfuric acid monomer concenterations in nucleation studies

K. Neitola[1], D. Brus[1,2], U. Makkonen[1], M. Sipilä[3], R. L. Mauldin III[3,4], N. Sarnela[3], T. Jokinen[3], H. Lihavainen[1], and M. Kulmala[3]

[1]Finnish Meteorological Institute, Erik Palménin aukio 1, P.O. Box 503, 00100 Helsinki, Finland
[2]Laboratory of Aerosol Chemistry and Physics, Institute of Chemical Process Fundamentals Academy of Sciences of the Czech Republic, Rozvojová 135, 165 02 Prague 6, Czech Republic
[3]Department of Physical Sciences, University of Helsinki, P.O. Box 64, 00014 Helsinki, Finland
[4]Institute for Arctic and Alpine Research, University of Colorado, Boulder, CO 80309, USA

Correspondence to: K. Neitola (kimmo.neitola@fmi.fi)

Received: 15 August 2014 – Published in Atmos. Chem. Phys. Discuss.: 13 October 2014
Revised: 26 January 2015 – Accepted: 24 February 2015 – Published: 28 March 2015

Abstract. Sulfuric acid is known to be a key component for atmospheric nucleation. Precise determination of sulfuric-acid concentration is a crucial factor for prediction of nucleation rates and subsequent growth. In our study, we have noticed a substantial discrepancy between sulfuric-acid monomer concentrations and total-sulfate concentrations measured from the same source of sulfuric-acid vapor. The discrepancy of about 1–2 orders of magnitude was found with similar particle-formation rates. To investigate this discrepancy, and its effect on nucleation, a method of thermally controlled saturator filled with pure sulfuric acid (97 % wt.) for production of sulfuric-acid vapor is applied and rigorously tested. The saturator provided an independent vapor-production method, compared to our previous method of the furnace (Brus et al., 2010, 2011), to find out if the discrepancy is caused by the production method itself. The saturator was used in a H_2SO_4–H_2O nucleation experiment, using a laminar flow tube to check reproducibility of the nucleation results with the saturator method, compared to the furnace. Two independent methods of mass spectrometry and online ion chromatography were used for detecting sulfuric-acid or sulfate concentrations. Measured sulfuric-acid or total-sulfate concentrations are compared to theoretical predictions calculated using vapor pressure and a mixing law. The calculated prediction of sulfuric-acid concentrations agrees very well with the measured values when total sulfate is considered. Sulfuric-acid monomer concentration was found to be about 2 orders of magnitude lower than theoretical predictions, but with a temperature dependency similar to the predictions and the results obtained with the ion-chromatograph method. Formation rates are reproducible when compared to our previous results with both sulfuric-acid or total-sulfate detection and sulfuric-acid production methods separately, removing any doubts that the vapor-production method would cause the discrepancy. Possible reasons for the discrepancy are discussed and some suggestions include that the missing sulfuric acid is in clusters, formed with contaminants found in most laboratory experiments. One-to-two-order-of-magnitude higher sulfuric-acid concentrations (measured as total sulfate in this study) would contribute to a higher fraction of particle growth rate than assumed from the measurements by mass spectrometers (i.e. sulfuric-acid monomer). However, the observed growth rates by sulfate-containing vapor in this study does not directly imply a similar situation in the field, where sources of sulfate are much more diverse.

1 Introduction

Secondary particle formation by gas-to-liquid conversion is widely recognized as an important source of aerosol particles in the atmosphere worldwide (Weber et al., 1996; Kulmala et al., 2004; Spracklen et al., 2006). These particles may grow to larger sizes and affect the radiative balance of the Earth by scattering and absorbing incoming radiation (Feingold and

Siebert, 2009). Model calculations and observations suggest that new particle formation events with subsequent growth can contribute a substantial amount to cloud condensation nuclei (CCN) concentrations, which can alter the lifetime and albedo of clouds (Lihavainen et al., 2003, 2009; Merikanto et al., 2009). Furthermore, aerosols can reduce visibility and have potential health effects (Davidson et al., 2005).

Significant effort has been made by field measurements and laboratory studies, together with computer simulations, to understand the particle-formation mechanism itself and the atmospheric conditions involved in the gas-to-liquid conversion. Despite such efforts and numerous results, the underlying mechanism is not yet found.

It is widely accepted that sulfuric acid plays a key role in atmospheric nucleation (Kulmala et al., 2006; Sipilä et al., 2010; Brus et al., 2011; Kirkby et al., 2011). Binary nucleation of sulfuric acid and water (Vehkamäki et al., 2002; Yu, 2006; Kirkby et al., 2011), ternary nucleation involving also ammonia and/or amines (Ball et al., 1999; Korhonen et al., 1999; Napari et al., 2002; Benson et al., 2009; Berndt et al., 2010; Kirkby et al., 2011; Zollner at al., 2012) and ion-induced nucleation (Lee et al., 2003; Lovejoy et al., 2004; Yu et al., 2008, 2010; Nieminen et al., 2011) have been suggested as possible mechanisms for nucleation to occur in the atmosphere. Ions have been shown to lower the thermodynamic potential of nucleation (Arnold, 1980; Winkler et al., 2008; Kirkby et al., 2011), but the role of ions in nucleation occurring in the atmospheric boundary layer has been shown to be minor (Manninen et al., 2010; Paasonen et al., 2010, Kerminen et al., 2010; Hirsikko et al., 2011).

Recently several laboratory studies have been conducted concerning the role of sulfuric acid in atmospheric nucleation (e.g. Benson et al., 2008, 2011; Young et al., 2008; Berndt et al., 2008, 2010; Brus et al., 2010, 2011; Sipilä et al., 2010; Kirkby et al., 2011; Zollner et al., 2012) with different methods of producing the gas-phase sulfuric acid: with their own advantages and disadvantages. For example, the evaporation method of weak sulfuric-acid solution used by Viisanen et al. (1997) and Brus et al. (2010, 2011) introduces a thermal gradient. Production of sulfuric acid with a SO_2+ OH reaction is used in most of the experiments, since it is similar to that observed in atmosphere (e.g. Benson et al., 2008; Berndt et al., 2008, 2010; Sipilä et al., 2010; Kirkby et al., 2011). The SO_2 oxidation method involves the use of UV light to produce OH radicals. The excess OH must be removed so that it does not disturb the nucleation process itself (Berndt et al., 2010). Another way is to have excess SO_2, so that all the OH reacts rapidly with SO_2; but for the calculation of the produced H_2SO_4 concentration, the exact concentration of OH produced must be known (Benson et al., 2008). Ball et al. (1999) and Zollner et al. (2012) produced sulfuric-acid vapor by saturating N_2 flow in a saturator, containing pure ($\sim$96 and $\sim$98 %, respectively) sulfuric acid. Ball et al. (1999) varied the temperature of the saturator, whilst Zollner et al. (2012) kept the saturator at constant temperature (303 K) and varied the carrier-gas flow rate to change the sulfuric-acid concentration.

As stated by others in literature (e.g. Benson et al., 2011; Brus et al., 2011; Kirkby et al., 2011), contaminants are present in most laboratory nucleation studies. These contaminants arise from different sources, such as from the water used for humidifying the carrier gas or from the carrier gas itself which contains trace levels of contaminants. It is almost impossible to remove these contaminants, which most probably affect the nucleation process itself.

Brus et al. (2011) reported a discrepancy in sulfuric-acid mass-balance between a known concentration of weak sulfuric-acid solution introduced to the experimental setup and a measured sulfuric-acid concentration, even though correction for wall losses and losses to particle-phase was applied, a 1.5 order-of-magnitude difference in sulfuric acid concentration was found (see Fig. 5 in Brus et al., 2011). A similar, large discrepancy between measured sulfuric-acid monomer concentrations and total-sulfate concentration was observed in the present study. To investigate the reason for this discrepancy, we applied a thermally controlled saturator (e.g. Wyslouzil et al., 1991; Ball et al., 1999) to produce sulfuric-acid vapor. The output of the saturator was tested with two independent detection methods (mass spectrometry and ion chromatography) before using the saturator in a H_2SO_4—H_2O nucleation study in a laminar flow tube.

Applying the saturator as the source of the sulfuric-acid vapor made it possible to compare the saturator to the furnace, which was used as the source of the sulfuric acid previously (Brus et al., 2010, 2011) and eliminate the production method as a reason for the discrepancy. The flow-tube measurements with the saturator and the two sulfuric-acid or total-sulfate detection methods were conducted to check reproducibility of particle formation rates between the saturator and the furnace, with similar observed sulfuric-acid or total-sulfate concentrations. The measured sulfuric-acid or total-sulfate concentrations were compared and the total losses of sulfuric acid or sulfate were determined for both mass spectrometers and the ion chromatograph. The level of ammonia contaminant in the system was determined with the ion-chromatograph method.

2 Experimental

The measurement setup presented here is partially introduced in Brus et al. (2010); only the main principle of the method, and the most substantial changes, are described here. The setup for testing the output of the saturator with two independent sulfuric-acid or total-sulfate detection methods is described. Shortly presented is the instrumentation for sulfuric-acid or total-sulfate and detection of freshly formed particles.

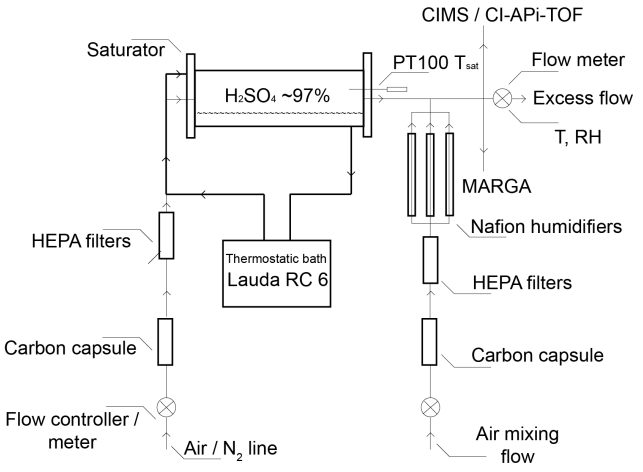

Figure 1. Schematic figure of the setup for testing the saturator.

2.1 Saturator

The saturator was a horizontally placed cylinder made of iron with a Teflon insert inside the cylinder (inner diameter, I.D., of 5 cm). It was thermally controlled with a liquid-circulating bath (LAUDA RC 6) and the temperature was measured just above the liquid surface with a calibrated PT100 probe (accuracy ± 0.05 K) inserted from the outlet side of the saturator (Fig. 1). The saturator was filled with 150–200 mL of pure sulfuric acid (~ 97 % wt., Baker analyzed). H_2SO_4 vapor was produced by flowing purified, dry, particle-free carrier gas through the saturator in the range of 0.05–1 liters per minute (Lpm) saturating the flow with vapor according to the temperature of the saturator. Carrier gas flows were purified in all experiments first with activated carbon capsules (Pall Corp., USA) to remove all organic vapors via diffusion to the surfaces and after with a HEPA filters (Pall Corp. USA) to remove any particles left in the flow. The saturator flow was thermally controlled to the same temperature as the saturator before entering it, to ensure temperature stability inside the saturator.

The theoretical prediction of sulfuric-acid vapor concentration was calculated using the equation for vapor pressure from Kulmala and Laaksonen (1990) which uses the measurements by Ayers et al. (1980) and theoretically extrapolates the vapor pressure to lower range of temperatures used in this study:

$$\ln p = \ln p_0 + \frac{\Delta H_v(T_0)}{R} \times \left[-\frac{1}{T} + \frac{1}{T_0} + \frac{0.38}{T_c - T_0} \times \left(1 + \ln \frac{T_0}{T} - \frac{T_0}{T} \right) \right], \quad (1)$$

where p is the vapor pressure (atm), $p_0 = -(10\,156 / T_0) + 16.259$ atm (Ayers et al., 1980), T is the temperature, T_c is critical temperature, 905 K, and T_0 is chosen to be 360 K so $\Delta H_v\ (T_0) / R = 10\,156$. See Kulmala and Laaksonen (1990) for more details. Here the predicted sulfuric-acid concentration depends only on saturator temperature, flow rate through the saturator and mixing flow. Measured sulfuric-acid or total-sulfate concentration is compared also to empirical fit by Richardson et al. (1986):

$$\ln p = 20.70 - \frac{9360}{T}. \quad (2)$$

The fit is made to their measurement data in the temperature range of 263.15–303.15 K, which suits the temperature range of the present study.

2.2 Setup for testing saturator with mass spectrometers and online ion chromatograph

The saturator was tested in two different tests. First with mass spectrometers: a chemical ionization mass spectrometer (CIMS) (Eisele and Tanner, 1993; Mauldin et al., 1998; Petäjä et al., 2009) and an atmospheric pressure interface time of flight mass spectrometer, (CI-Api-TOF, Tofwerk AG, Thun, Switzerland and Aerodyne Research Inc., USA; Junninen et al., 2010) with a chemical ionization inlet similar to the CIMS (Jokinen et al., 2012). A second test was done with the instrument for measuring aerosols and gases (MARGA, Metrohm Applikon Analytical BV, Netherlands; ten Brink et al., 2007). Both measurements were performed with the same setup (Fig. 1). The flow from the saturator (0.5 Lpm) was mixed with another flow of the same gas (20 or 40 Lpm) after the saturator to meet the inlet flows of the instruments. The relative humidity (RH) was set by 2 or 3 Nafion humidifiers (MD-series, Perma pure, USA) and monitored from the excess flow. The design of the inlet system for mixing the different flows and flow schematics to the instruments can be found in the Supplementary Material (Fig. S2 in the Supplement). Different configurations after the mixing were tested, and no difference in the observed concentration was found. The temperature of the saturator was increased in 5-degree steps from approximately 273 to 303 K (MARGA) and 313 K (CIMS and CI-Api-TOF) in order to increase the sulfuric-acid concentration. The temperature was kept constant from 2 to 8 h in order to achieve a steady state. The measured sulfuric-acid monomer concentrations and total-sulfate concentrations were compared to theoretical values calculated from the vapor pressure of sulfuric acid using Eqs. (1) and (2).

2.3 Flow-tube setup for nucleation measurements

The flow-tube setup consists of four main parts: a saturator, a mixing unit, a flow nucleation chamber and detection of sulfuric acid or total sulfate and particles (Fig. 2). The sulfuric-acid vapor is produced in the saturator and turbulently mixed with clean, particle-free carrier gas in the mixing unit. Particles formed inside the saturator are lost in the 1 m long, thermally controlled Teflon tube (I.D. 4 mm) before the mixer,

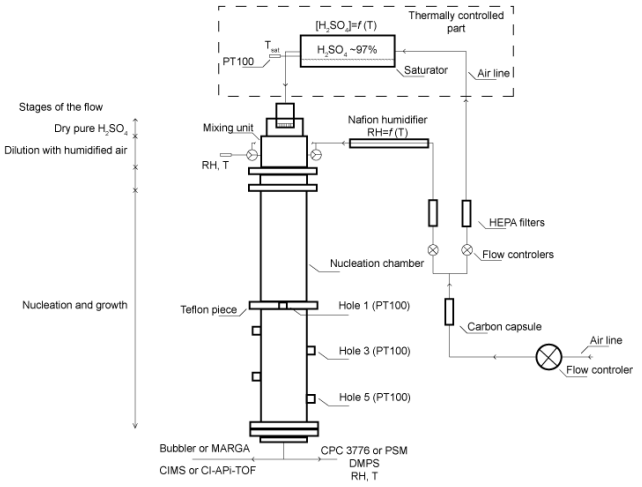

Figure 2. Flow-tube setup.

by diffusion and by turbulent mixing in the mixer. After the mixing unit, nucleation and subsequent growth take place in the laminar flow chamber. The flow chamber consists of two 100 cm long stainless steel cylinders (I.D. 6 cm) connected with a Teflon piece (height 3.5 cm, I.D. 6 cm), positioned vertically and thermally controlled with a liquid circulating bath (LAUDA RC 6). One of the 100 cm long parts of the flow chamber has four holes on the sides every 20 cm from the beginning of the chamber. The 3.5 cm Teflon connector between the two 100 cm flow-tube pieces also has a hole (see Fig. 2). These holes are used to continuously measure temperature in the flow tube with PT100 probes to ensure constant desired nucleation temperature. The RH of the mixing flow is controlled by 2 or 3 Nafion humidifiers. RH and temperature are measured also at the end of the tube with Vaisala HMP37E and humidity data processor Vaisala HMI38. Both saturator and mixing flow of the tube are controlled by a mass flow-rate controller (MKS type 250) with an accuracy of ± 3 %. Flow rates through the saturator for nucleation measurements were kept at 0.13–0.27 Lpm. The mixing flow was kept at approximately 11 Lpm.

2.4 H_2SO_4 monomer, sulfate and particle detection

Gas phase sulfuric-acid monomers were measured with CIMS or CI-Api-TOF. The CI-inlet used in both instruments works as follows: the sulfuric-acid molecules are ionized in ambient pressure via proton transfer between nitrate ions (NO_3^-) and sulfuric acid molecules (H_2SO_4). The nitrate ions are produced from nitric acid with radioactive ^{241}Am-source and mixed in a controlled manner in a drift tube, using a concentric sheath and sample flows together with electrostatic lenses.

After the ionization in the inlet, the instruments differ from each other. In the CIMS, sample flow is dried using a nitrogen flow to dehydrate the molecules before entering the vacuum system and detection in the quadrupole mass spectrometer. In the CI-Api-TOF, a flow rate of 0.8 Lpm is guided through a critical orifice. The ions are guided through the differentially pumped Atmospheric pressure interface (Api) and finally to the TOF for detection according to the ions' mass-to-charge ratio.

The monomer concentration is determined by the ratio of the resulting ion signals (HSO_4^- and $HSO_4^- \cdot HNO_3$) and the reagent ion signals (NO_3^-, $HNO_3 \cdot NO_3^-$ and $(HNO_3)_2 \cdot NO_3^-$). This ratio is then multiplied by the instrument-dependent calibration factor in both instruments. The calibration factor used here was 5×10^9 for both instruments. Neither CIMS nor CI-Api-TOF was calibrated using the saturator setup, but instead before the experiments using the standard calibration procedure of oxidation of SO_2 with OH (Kürten et al., 2012). For more information about the calibration of CIMS, see Berresheim et al. (2000), Petäjä et al. (2009), Zheng et al. (2010) and Kürten et al. (2012). The nominal sample flow rate of these instruments is ~ 10 Lpm. We considered only the monomer concentration, although detection of dimers and even larger clusters of pure sulfuric acid is possible with CI-Api-TOF. This was done because the dimer concentration was always in the magnitude of ~ 1 % of monomer concentration and the trimer concentration was in the magnitude of ~ 1 % of the dimer concentration, continuing with similar concentration ratio towards larger clusters (e.g. Jokinen et al., 2012). The charging efficiency might not be the same for these clusters as it is for monomer. This would cause the calibration factor to change and the calculated concentration to be erroneous. The uncertainty in the resulting monomer concentration is estimated to be a factor of ~ 2. The nominal lower detection limit of CIMS and CI-Api-TOF is estimated to be 5×10^4 cm^{-3}, and the upper limit is approximately 10^9 cm^{-3} for both instruments. At this high concentration, the primary ions start to deplete causing the calibration factor to change.

The total-sulfate concentration was measured with an online ion chromatograph MARGA 2S ADI 2080. MARGA is able to detect five gases in the gas phase (HCl, HNO_3, HONO, NH_3, SO_2) and eight major inorganic species in aerosol phase (Cl^-, NO_3^-, SO_4^{2-}, NH_4^+, Na^+, K^+, Mg^{2+}, Ca^{2+}). The sample flow is ~ 16.7 Lpm. From the sample flow, all (more than 99.7 %) of water-soluble gases are absorbed into a wetted rotating denuder (WRD). Based on different diffusion velocities, aerosols pass the WRD and enter a steam-jet aerosol collector (SJAC) (Slanina et al., 2001). In the SJAC, conditions are supersaturated with water vapor, which condenses onto particles and the particles thus collect at the bottom of the SJAC. Sample solutions are drawn from the WRD and the SJAC into syringes (25 mL) and are analyzed one after another, once an hour. Samples are injected in cation and anion chromatographs with an internal standard (LiBr). Components are detected by conductivity measurements. The detection limits are 0.1 µg m^{-3} or better.

For more information about the instrument, see Makkonen et al. (2012).

In our previous study (Brus et al., 2010), the total-sulfate concentration was measured using the method of bubblers, where a known flow rate from the flow tube was bubbled through alkaline solution, thus trapping sulfate. This solution was then analyzed using offline ion chromatography. See Brus et al. (2010) for details. The method of bubbler is analogous to the MARGA, and the main difference is that MARGA is an online method, whilst bubbler is an offline method.

The total-particle number concentration was measured with a particle size magnifier (PSM, Airmodus Oy, Finland, Vanhanen et al., 2011, coupled with CPC TSI model 3772) and with Ultra-Fine CPC's (UFCPC, TSI models 3776, 3025A) with cut-off mobility diameters of ~ 1.5 and ~ 3 nm, respectively. A differential mobility particle sizer (DMPS) was used to measure the particle number size distribution from 3 to ~ 250 nm in a closed-loop arrangement (Jokinen and Mäkelä, 1997) using a blower to measure the wet size of the particles. The DMPS was run with a sheath flow of ~ 11 Lpm and sample flow of 1.5 Lpm in the short HAUKE-type Differential Mobility Analyzer (DMA). The DMA was coupled with UFCPC (TSI model 3025A) and with a bipolar radioactive (^{63}Ni) neutralizer. The charging efficiencies were calculated following the parameterization of Wiedensohler and Fissan (1991). The RH of the sheath flow was monitored to ensure that it was same as the RH in the chamber.

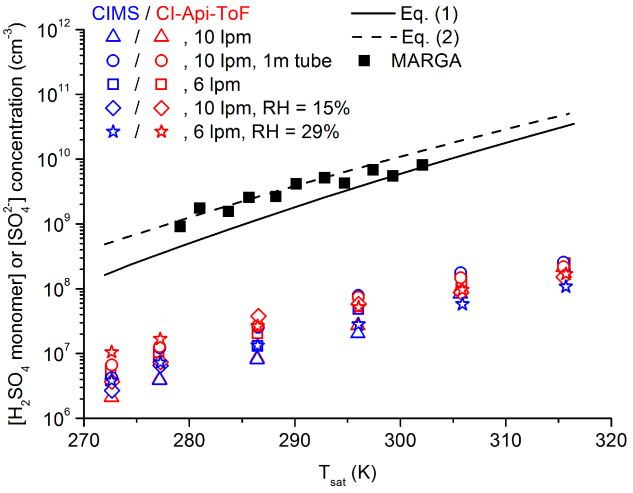

Figure 3. Measured sulfuric-acid monomer [H_2SO_4 monomer] concentration and total-sulfate [SO_4^{2-}] (black squares) concentrations together with predicted values by Eqs. (1) and (2) as a function of saturator temperature T_{sat}. Saturator flow rate is $Q_{sat} = 0.5$ Lpm and mixing flow rates were 40 Lpm (dry for CIMS and CI-Api-TOF and RH 15 %) and 20 Lpm (MARGA and RH 29 %). CIMS (blue markers) and CI-Api-TOF (red markers) have been tested with 6 and 10 Lpm (nominal) inlet total flow rates and also with an extra 1 m Teflon tubing after saturator.

3 Results

To quantify the sulfuric acid input for flow-tube nucleation measurements, the saturator output was tested in two experiments: first with CIMS and CI-Api-TOF and second with MARGA. After the tests, nucleation measurements of H_2SO_4–H_2O system were conducted. This enabled direct comparison with the sulfuric-acid production method used in our previous studies (Brus et al., 2010, 2011), so that the production method can be discounted as a reason for the discrepancy. Presented values from CIMS, CI-Api-TOF and MARGA measurements are residual, i.e. measured values at the end of the flow tube accounting for dilutions, if not otherwise mentioned to be different.

3.1 Test of the saturator

Results of the saturator test are presented in Fig. 3 as measured sulfuric-acid or total-sulfate concentrations and predicted values by Eqs. (1) and (2) as a function of temperature of the saturator. The mixing flows were 40 (dry and RH 15 %) or 20 Lpm (for RH 29 %) for CIMS and Api-TOF and 20 Lpm (only dry conditions) for MARGA measurements. Tests with MARGA were performed with dry conditions, since it was noticed that the RH did not have any influence on the results from the tests with mass spectrometers. MARGA uses supersaturated conditions to grow the particles and collect them in the SJAC, hence initial RH is not expected to have any influence. Saturator flow rate was 0.5 Lpm. Mass spectrometers were tested in dry and humid conditions. Dry experiments were run with two mass-spectrometer inlet flow rates (6 and 10 Lpm) and with extra 1 m (I.D. 4 mm) Teflon tubing between the saturator and the mixing unit, to test the effect of wall losses. Humidified experiments were done with two inlet flow rates (6 Lpm for RH 29 % and 10 Lpm for RH 15 %). MARGA experiments were conducted in dry conditions.

The total-sulfate concentration measured with MARGA (black squares) fits the prediction by Eq. (2) (dashed line) very well and the prediction by Eq. (1) (solid line) slightly underestimates the measured total-sulfate concentration. MARGA has a relatively fast inlet flow rate (~ 16.7 Lpm) so inlet losses are low; however, with increased temperature of the saturator, diffusional losses are visible.

Sulfuric-acid monomer concentrations measured with CIMS and CI-Api-TOF fit each other very well, but they show 1–2-order-of-magnitude lower concentrations than predicted by Eqs. (1) and (2) and measured total sulfate with MARGA. The slope is similar to the predictions and to the points measured with MARGA. The dimer concentration was always approximately 1 to 10 % (increasing with increasing saturator temperature) of the monomer concentra-

tion and trimer approximately 1 % of the dimer concentration (see Supplement, Fig. S5).

Relative humidity did not have any substantial effect on the measured values by CIMS and CI-Api-TOF. RH can affect the wall losses by preventing the sulfuric acid's evaporation from the inlet walls, since the vapor pressure of water is several orders of magnitude higher than that of the sulfuric acid. The predictions by Eqs. (1) and (2) do not consider relative humidity, since the flow through the saturator is always dry. The relative humidity of the mixing flow causes the sulfuric acid molecules to get hydrated since sulfuric acid is very hygroscopic; but because the results from humid and dry measurements are very similar, CIMS and CI-Api-TOF can be considered to measure well in humid conditions as well. The effect of RH is discussed in Eisele and Tanner (1995) and our results agree with the discussion there.

A change of the nominal inlet flow rate of CIMS and CI-Api-TOF did not have a large effect. The inlet lines were short (~ 20 cm) in the saturator tests, so the wall losses due to lower inlet flow rate did not play any significant role. Using instruments with a lower flow rate might alter the measured concentration, because the calibration factor is acquired with inlet flow rate of 10 Lpm.

Extra saturator tests with mass spectrometers were done using three different carrier gas purities (N_2 6.0, N_2 5.0 and pressurized air) to check if the carrier gas used in our experiments (pressurized air) was dirtier than the purest commercial ones. Two different purity sulfuric acids (~ 97 and 100 %) were tested also to check if the purity of the acid itself has an influence. Changing the carrier gas or the sulfuric acid purity did not affect the observed sulfuric-acid concentration (see Supplement, Figs. S3 and S4). The measured sulfuric-acid monomer concentration was 1–2 orders-of-magnitude lower than the prediction by Eq. (1). Tests with different saturator flow rates (0.05–2 Lpm) showed that with flow rates below 0.1 Lpm, diffusion losses dominated, thereby causing the measured concentration to decrease as a function of the saturator temperature. Above 0.15 Lpm, the observed results behaved as expected. The measured cluster distributions (monomer, dimer and trimer) with different carrier-gas purity were constant through the measured saturator flow rate range (Fig. S5 in the Supplement). The ratios between monomer-to-dimer and dimer-to-trimer were between 1 : 10 and 1 : 100 with all carrier gases. From these results it is evident that the carrier gas used in our studies does not contain more contaminants than the purest commercially available pure gases. CI-Api-TOF mass spectra observed with different carrier gases were investigated further, to find the missing sulfuric acid. A large number of peaks were found to correlate with mass 97 (HSO_4^-), which is the ionized sulfuric-acid monomer, with all carrier gases. The number of these peaks increased as a function of the saturator temperature, suggestive that the sulfuric acid forms clusters with contaminant substances (Supplement, Sect. 6, Figs. S6–S8). The correlating peaks in Figs. S6–S8 in the Supplement are stick masses (i.e. rounded to the nearest integer), which means that many of those peaks have actually several peaks within them. This is shown in Figs. S9–S11 in the Supplement where the mass spectrum from CI-Api-TOF is zoomed in. Unfortunately, summing up all of these correlating peaks to calculate the total sulfuric acid concentration is not feasible, since these clusters are not identified (i.e. it is not known what molecules those clusters are composed of) and the sheer number of these peaks is overwhelming. For more details and discussion of the extra saturator tests, see Supplement.

3.2 Losses of sulfuric acid and sulfate in the flow tube

Total losses were not directly measured, but they were determined by comparing results from saturator tests with the results from nucleation measurements. The setup of the measurements was similar in both experiments except for the flow tube used in nucleation measurements. By accounting for the different mixing ratios of saturator flow rate and mixing flow rate, these measurements become comparable and the total losses in the flow tube can be determined. The total loss factor (TLF) includes wall losses and losses to the particle phase (nucleation and condensational losses).

Figure 4 presents the measured sulfuric-acid-monomer and total-sulfate concentration from the saturator tests (squares) and nucleation measurements (stars) as a function of the saturator temperature. Saturator tests were done in dry conditions and nucleation measurements in RH 30 %. An inlet pipe is used to connect the mass spectrometer to the flow tube. Brus et al. (2011) state that the wall loss factor (WLF) in the inlet pipe of length $100 + 22$ cm is $\mathrm{WLF_{inlet}} = \sim 4$. This factor, together with the mixing ratios, was accounted for to make the data sets directly comparable.

A linear fit was applied to the data and TLF values were determined from the ratio of the fits. The TLF values were determined for a saturator temperature range of 286–300 K for CIMS and 284–297 K for MARGA depending on the measurement range of the data. The average TLF values are 14.2 ± 4.2 for CIMS and 10.0 ± 1.2 for MARGA. The R^2 values for the fits are 0.96, 0.87, 0.90 and 0.61 for CIMS saturator test, CIMS nucleation measurement, MARGA saturator test and MARGA nucleation measurement, respectively.

From Fig. 4, it is evident that wall losses are not the only losses affecting the measured concentrations since the trends in the fits for nucleation measurements are less steep than the ones from saturator tests. The losses to the particle phase also affect the situation. The maximum losses of sulfuric acid to particle phase are calculated using the DMPS data measured at the end of the nucleation chamber only. The total volume of the particles is calculated within the size distribution assuming that the particles are composed only of pure sulfuric acid with density of $1.84\,\mathrm{g\,cm^{-3}}$. The losses of sulfuric acid to particles range from 0 % (dry conditions, $T_{\mathrm{sat}} = 273$ K) up to maximum of 1.4 % (RH = 30 %, $T_{\mathrm{sat}} = 292$ K) of the total sulfate concentration. Higher saturator temperature increases

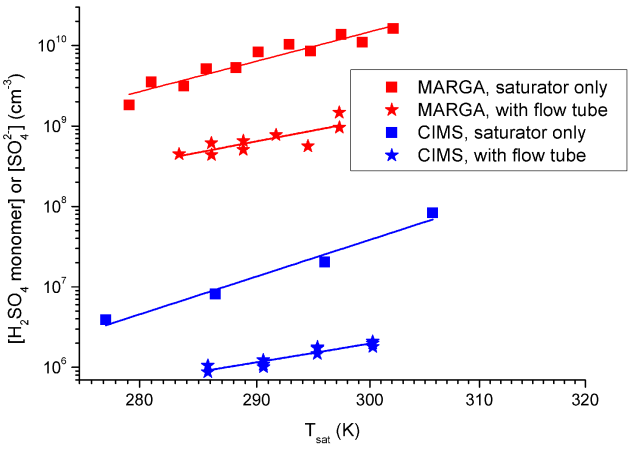

Figure 4. Comparison of MARGA and CIMS data between test with saturator only (dry conditions, squares) and with saturator and flow tube (RH ∼ 30 %, stars). Different flow rates through saturator have been accounted for. Average total loss factors are $\mathrm{TLF_{MARGA}} = 10.0 \pm 1.2$ and $\mathrm{TLF_{CIMS}} = 14.2 \pm 4.2$. See text for details.

the number and the diameter of the particles, and relative humidity increases the diameter of the particles. The losses to the particle phase are substantial at the highest values of saturator temperature, but this estimate is the maximum limit, since the particles are not composed only of pure sulfuric-acid molecules. Contaminants from the flow condense to the particle phase or bond with sulfuric acid. When using humid conditions, sulfuric-acid particles uptake water since sulfuric acid is very hygroscopic. At the highest temperature of the saturator, the size distribution unfortunately extends out of the DMPS range (3–250 nm), thus conversely underestimating the losses. Losses to the clusters smaller than the cut-off size of the particle counters are substantial. The maximum losses to the particle phase have been calculated for each of the saturator temperature values and plotted with the measured monomer and total sulfate concentrations together with the prediction from Eq. (1) in Fig. S1 in the Supplement. Even summing up the measured monomer concentration and the losses to the particle phase leaves the summed total concentration at least 1 order of magnitude lower than the measured total sulfate and the prediction by Eq. (1).

3.3 Nucleation measurements

Formation rates J of H_2SO_4–H_2O nucleation were measured in the range from 0.1 to $\sim 300\,\mathrm{cm^{-3}\,s^{-1}}$ with sulfuric-acid monomer concentration approximately from 5×10^5 to $10^7\,\mathrm{cm^{-3}}$ or in total sulfate concentration approximately from 4×10^8 to $3 \times 10^9\,\mathrm{cm^{-3}}$. Formation rates are usually reported as $J_{1.5}$ or J_3 (cut-off sizes of the particle counters are 1.5 nm for PSM and 3 nm for UFCPC TSI models 3776 and 3025) as discussed in Kulmala et al. (2012). However, particles measured at the end of our flow tube were almost always in the range of 8–20 nm, so we report formation rates as they were determined with our particle counters. The purpose of these nucleation measurements is to be able to compare the formation rates and the sulfuric-acid or total-sulfate concentrations, between the two sulfuric-acid-vapor-production methods. The results are discussed below.

Figure 5 presents DMPS and CIMS data for one cycle of saturator temperatures. (a) presents the number size distribution as a function of time, (b) presents the total particle number concentration, (c) shows the hourly averaged sulfuric-acid monomer concentration with standard deviation as the error bars, and (d) shows hourly averaged saturator temperature. One can see from Fig. 5a and b, that when the temperature of the saturator changes, the number concentration and the number size distribution are not stable immediately. The sulfuric-acid concentration slightly overshoots at the beginning whilst the system stabilizes to steady state. The first hour of averages from each of the saturator temperatures was excluded to ensure only steady-state data (std(T) = ±0.05 K) were included in the averages. When a new cycle started, the T_{sat} dropped from the maximum value (∼ 315 K) to the minimum (273 K), causing a long period of unstable data, and the first 2 h were excluded from the beginning of the cycle. In panel (a) in Fig. 5, nucleation is the main process below temperature of ∼ 290 K and growth takes over at higher temperatures. This can be seen as the bimodal distribution at highest saturator temperatures.

Figures 6 and 7 present the number concentration N_{exp} (panel a), geometric mean diameter D_{p} (panel b) and apparent formation rate J (panel c) of freshly nucleated particles with sulfuric-acid monomer concentration [H_2SO_4 monomer] or total sulfate [SO_4^{2-}] (panel d) as a function of saturator temperature T_{sat} for nucleation temperature of 298 K with several different relative-humidity values (Fig. 6) and saturator flow rates (Fig. 7). The formation rate is reported the observed particle concentration N_{exp} divided by the residence time τ.

From Fig. 6, it is evident that all measured variables behave as expected as a function of the saturator temperature, except for the apparent saturation of the observed particle concentration (and hence, the formation rate). PSM was coupled with the TSI model 3772 CPC's, which has an upper limit of $10^4\,\mathrm{cm^{-3}}$ for the particle concentration. This caused the observed particle concentration to saturate in Fig. 6, even though the particle concentration was confirmed to increase to higher values by DMPS data (not shown in the Fig. 6). Coagulation has a minor effect on the particle number due to a short residence time ($\tau = 30$ s) and relatively low particle concentration (maximum concentration of $1.2 \times 10^4\,\mathrm{cm^{-3}}$ from DMPS data). The relative humidity affects mostly the diameter of the particles, but also decreasing RH decreases the formation rate if similar sulfuric-acid concentration is considered. A lower formation rate with decreased RH might be caused by the diminishing of the particle diameter below the detection limit of the UFCPC (TSI model 3776). In

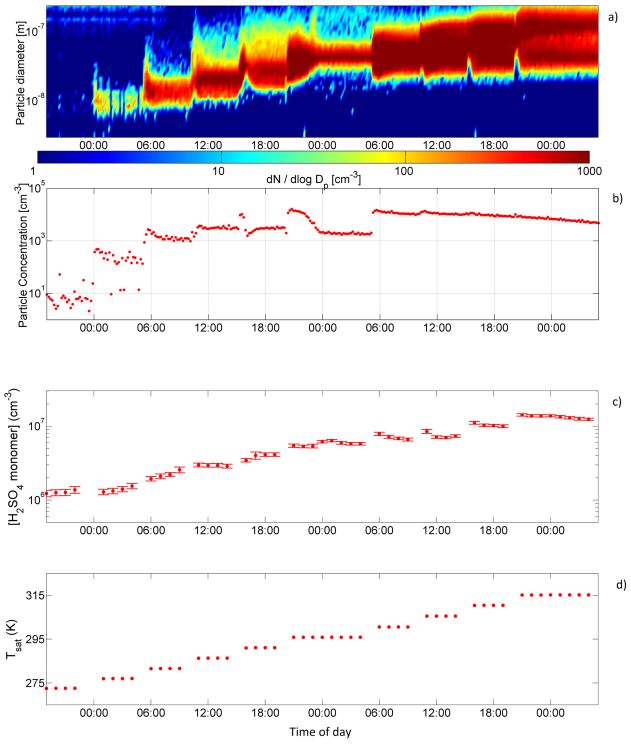

Figure 5. DMPS and CIMS data from one T_{sat} cycle. **(a)** shows the number size distribution, **(b)** shows the total number concentration from DMPS, **(c)** shows the CIMS-measured sulfuric-acid monomer concentration averaged over 1 h with standard deviation as error bars and panel **(d)** shows hourly averaged temperature of the saturator.

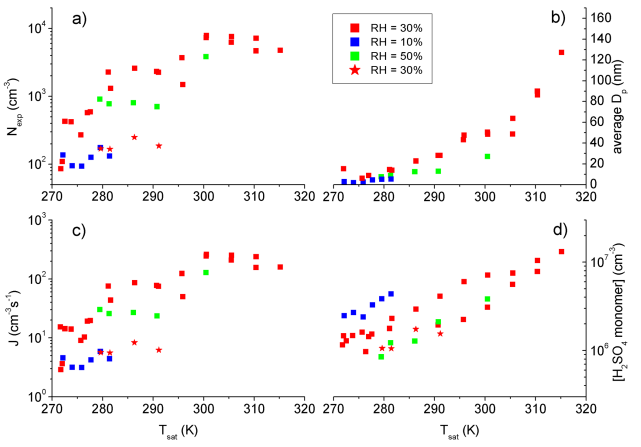

Figure 6. Number concentration N_{exp} **(a)** measured with PSM and TSI 3776, geometric-mean diameter D_p **(b)**, apparent formation rate J **(c)** of the freshly nucleated particles and sulfuric-acid monomer concentration measured **(d)** with CIMS (squares) or CI-Api-TOF (stars) with several relative humidity as a function of saturator temperature with saturator flow of 0.1 Lpm. All data are averaged over a period of constant saturator temperature excluding first hour to ensure steady-state. Stars are measured with CI-Api-TOF and squares with CIMS. All data are averaged over a period of constant saturator temperature (±0.05 K) extracting the first hour.

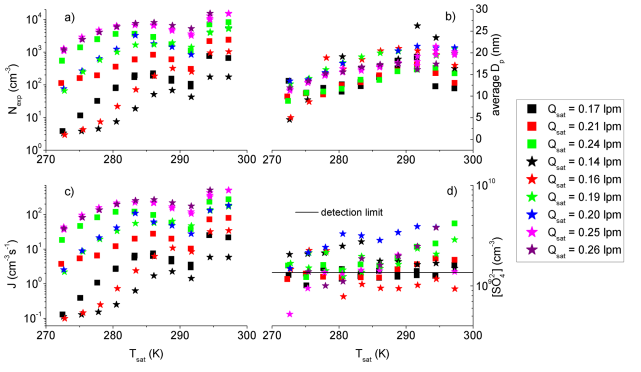

Figure 7. Number concentration N_{exp} **(a)** measured with TSI 3776, geometric mean diameter D_p **(b)**, formation rate J **(c)** of the freshly nucleated particles and total-sulfate concentration from MARGA **(d)** with detection limit of MARGA with several different saturator flow rates as a function of saturator temperature. Squares represent measurements under dry conditions, stars are measured with RH of ∼ 30 %. All data are averaged over a period of constant saturator temperature (±0.05 K) extracting the first hour.

Fig. 7, the squares present measurements during dry conditions and stars during RH of 30 %. Panel (d) shows also the detection limit of MARGA for total-sulfate concentration. The detection limit was determined from 20 h of measurements with saturator flow rate set to zero and averaged over the time period. The detection limit was 1.35×10^9 cm^{-3}. All the total sulfate concentrations measured below this detection limit were considered as erroneous and rejected from further analysis, even though these values are presented in Fig. 7. MARGA can be used with concentration columns to measure lower concentrations of species, but it was not available in this study.

From Fig. 7, one can see that all the variables responded in a similar manner as CIMS and CI-Api-TOF experiment (Fig. 6). As the temperature of the saturator approaches the temperature of the mixing unit (laboratory temperature, ∼ 294 K), the number concentration of particles decreases and starts to increase again when saturator temperature is greater than that of the mixing unit. This is an artefact of the setup.

The main difference between Figs. 6 and 7 is the maximum diameter reached. Due to the greater maximum saturator temperature (315 K) in the experiment with the mass spectrometers, the maximum diameter reached up to ∼ 130 nm compared to the ∼ 23 nm with the experiment with MARGA. The residence times in the flow tube are the same in both experiments (∼ 30 s). The measured sulfuric-acid monomer concentration is at typical atmospheric levels, but the growth rates are much higher: indicating higher concentration of sulfuric-acid-containing condensing vapor than the detected sulfuric-acid-monomer concentration by CIMS. The growth

is rather driven by the total sulfate, originating exclusively from the sulfuric acid inside the saturator, than the sulfuric-acid-monomer concentration.

To show the contribution of the sulfate to the growth rate, the model described in Škrabalová et al. (2014) was used to calculate the diameter (D_p) and growth rate (GR) of the particles. Measured sulfuric-acid monomer and total-sulfate concentrations (Figs. 6 and 7), RH 30 %) were multiplied by the TLFs to obtain the initial concentrations of vapor at the beginning of the flow tube. Diameter of 1.5 nm was chosen as the initial cluster size according to Kulmala et al. (2007). The model was used with three scenarios of particle neutralization by ammonia: (0) no neutralization, particles composed of sulfuric acid and water, (1) neutralization to ammonium bisulfate-water particles and (2) neutralization to ammonium sulfate-water particles. When accounting for the initial sulfuric-acid monomer concentration as an input, the resulting diameter (D_p) was always below 2 nm with growth rates (GR) ranging approximately from 1 to 15 nm h^{-1} as a function of the sulfuric-acid concentration (i.e. saturator temperature T_{sat}) with all scenarios. When total-sulfate concentration was used as an input, the resulting particle diameters and growth rates fit well with the measured particle diameters presented in Fig. 7 for all scenarios (see Supplement, Sect. 7 and Fig. S12).

3.4 Formation rates and comparison to our previous results

Figure 8 presents formation rates J of the H_2SO_4–H_2O system as a function of sulfuric-acid monomer concentration measured with CIMS at nucleation temperature of $T = 298$ K and RH of ~ 30 %. Sulfuric acid was produced with the method of furnace (red squares, Brus et al., 2011) and with saturator (the black squares, present study). The sulfuric-acid concentration for data from Brus et al. (2011) is presented here as residual concentration (i.e. at the end of the flow tube) so that these two measurements would be comparable. Brus et al. (2011) present their data as the initial concentration. Both data sets have almost identical slopes (1.3 and 1.2), and the formation rates J have a difference of a factor of 2. For the data set measured with the production method of the furnace, the residence time ($\tau = 15$ s) is defined as the time that the particles spend in the flow tube after the nucleation zone. The nucleation zone was experimentally determined (Brus et al., 2010) and confirmed with the computational fluid dynamics (CFD) model (Herrmann et al., 2010) to be in the middle of the flow tube in the measurements with the furnace, where a thermal gradient was present. For the saturator measurements (present work), the residence time ($\tau = 30$ s) was defined as the whole time the particles spend in the flow tube. The difference of the residence time is exactly a factor of 2. Formation rate is defined as the number concentration divided by the residence time, so these two sets of data lie on top of each other if the same residence time would have been used for formation-rate determination.

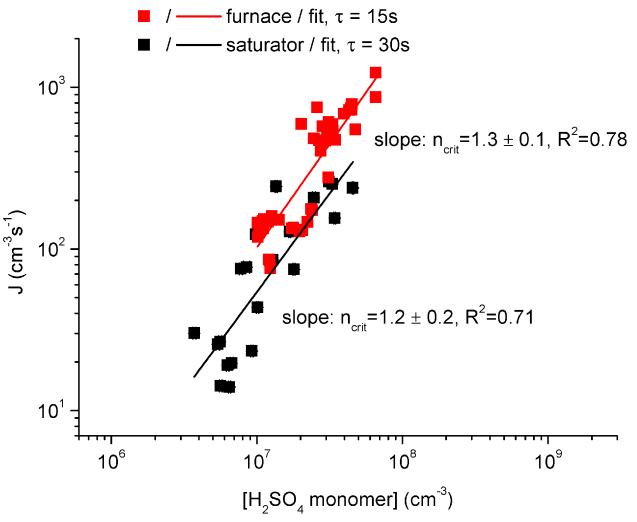

Figure 8. Formation rates J as a function of residual sulfuric-acid-monomer concentration [H_2SO_4 monomer] at $T = 298$ K and RH ~ 30 % measured using CIMS. In the first data set (red squares) sulfuric-acid vapor was produced with the furnace method, and the residence time was defined to be 15 s (Brus et al., 2011).

Figure 9 presents formation rates J of H_2SO_4–H_2O as a function of residual total sulfate concentration [SO_4^{2-}] at RH of ~ 30 % and at nucleation temperature of $T = 298$ K. Stars are the data from measurements where sulfuric-acid vapor was produced with the furnace and total sulfate measured with bubbler method (Brus et al., 2010). The residence time used in there was $\tau = 15$ s. Squares are total sulfate measured with MARGA in this study with different flow rates through the saturator, and the residence time was $\tau = 30$ s. All the points have the standard deviation as error bars. The detection limit of MARGA is also marked as a dashed vertical line. Formation rates are similar with both production methods. As previously, the factor-of-2 difference in the residence time increases the scatter between the two data sets.

Figures 8 and 9 show that apparent formation rates are reproducible with both sulfuric-acid production methods, with similar observed sulfuric-acid or total-sulfate concentrations. This eliminates the sulfuric-acid production method as a reason for the discrepancy between the measured monomer and total-sulfate concentrations. The data are more scattered in Fig. 9 due to the larger integration times used in MARGA and bubbler measurements. During several hours of integration time, a small change in flow rates can cause a substantial difference in the resulting concentration. MARGA data are close to the detection limit of the instrument, which also causes larger scatter.

Figure 10 shows a comparison of the apparent formation rates J as a function of residual sulfuric-acid monomer [H_2SO_4 monomer] concentration or total sulfate concentra-

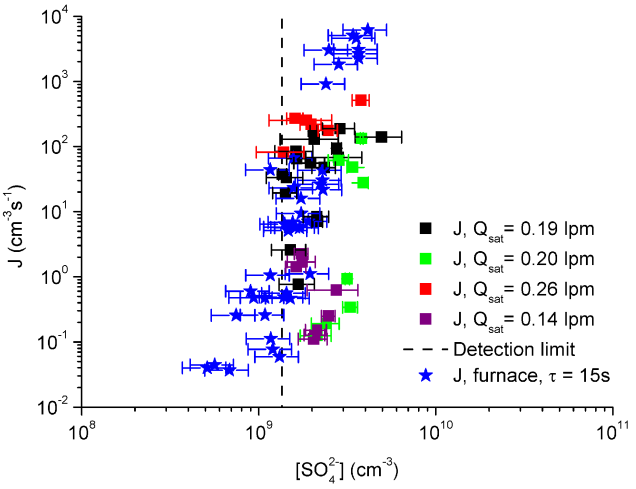

Figure 9. Formation rates J as a function of total-sulfate concentration $[SO_4^{2-}]$ measured with MARGA or bubbler with different saturator flow rates. MARGA's detection limit is marked with the dashed line. Relative humidity RH ∼ 30 % and nucleation temperature $T = 298$ K. Sulfuric-acid vapor was produced with the furnace method (Brus et al., 2010) for bubbler measurements and with the saturator method for MARGA.

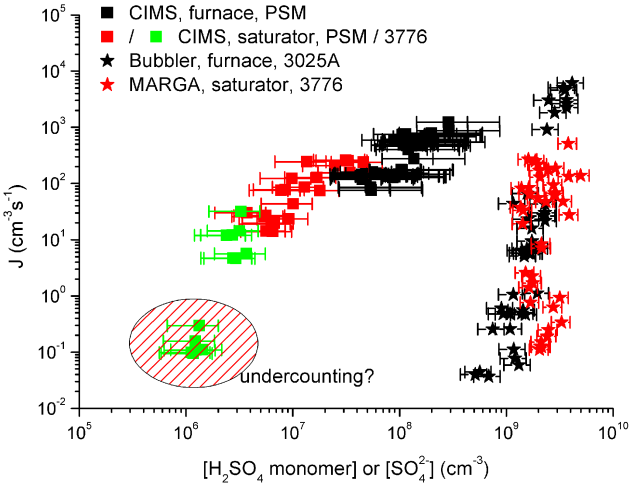

Figure 10. Comparison of formation rates J as a function of residual sulfuric-acid monomer concentration $[H_2SO_4]$ or total-sulfate concentration $[SO_4^{2-}]$ to our previous results. Conditions are similar ($T = 298$ K, RH ∼ 30 %). Note the factor-of-2 difference between the residence times between furnace and saturator measurements. Sulfuric-acid vapor was previously produced with the furnace method and total-sulfate concentration measured with the bubbler method (Brus et al., 2010).

tion $[SO_4^{2-}]$ from this study to our previous studies with the standard deviation as error bars. Note the difference of a factor of 2 between the residence times. Squares show values measured using mass spectrometers (PSM, red and black squares; TSI 3776, green squares). Stars are data measured using ion-chromatograph (i.e. total sulfate) methods with two different UFCPC's (TSI 3025A, black stars and TSI 3776, red stars). Figure 10 shows that the production method does not have substantial effect since the results lie on same line when comparing results obtained with mass spectrometers or MARGA and bubbler method. The conditions for all the measurements were similar ($T = 298$ K, RH ∼ 30 %).

The slope of the data measured using MARGA or bubblers is steeper than the slope of the results measured with mass spectrometers. There is a discrepancy of 1–2 orders-of-magnitude between sulfuric-acid monomer and total-sulfate concentration for similar formation rates. The UFCPC 3776 (green squares) was probably undercounting at the lowest sulfuric-acid concentrations. This can be seen in Fig. 10 where the lowest observed formation rates are not consistent with the rest of the data. This is probably caused by the small size of the particles at such low sulfuric-acid concentration ($1–2 \times 10^6$ cm^{-3}) (Sipilä et al., 2010).

The comparison to literature data was omitted in this manuscript since the formation rates in the present study are very similar to our previous results (Brus et al., 2010, 2011). However, for comparison and review of experimental data on sulfuric-acid nucleation, refer to Zollner et al. (2012) and Zhang et al. (2012).

3.5 Contaminants

In our previous study (Brus et al., 2011), an ion chromatograph was used to determine the background levels of ammonia and it was found that the background concentration was below the detection limit of the IC (500 pptv), accounting for the flow rates in the nucleation chamber. The concentration of background ammonia was measured with the MARGA system in this study. An average total concentration (gas and particle phase) of ammonia was 60 pptv for dry conditions and 126 pptv for RH 30 %, supporting our previous results. The concentration did not change as a function of saturator temperature; thus, it is assumed to originate from the purified, particle-free air used as carrier gas in all measurements and from the ultrapure water (Milli-Q, Millipore) used for humidification. The concentration for dry conditions is of the same order of magnitude as the concentration of total sulfate at the lowest (273 K) temperature of the saturator. When increasing the saturator temperature, the ratio of ammonia to total sulfate decreases from ∼ 1 : 1 to ∼ 1 : 10, or less, for dry conditions and from ∼ 3 : 1 to ∼ 1 : 5 for humid conditions. The extra saturator tests, mentioned in Sect. 3.1 and found in the Supplement, showed that the carrier gas used in this experiment was at least as pure as the purest gas available commercially (AGA, N_2, 6.0), which has impurities less than 1 ppm, including hydrocarbons less than 0.1 ppm. According to the results found in the Supplement, the actions taken to purify the carrier gas in these experiments were sufficient.

Nevertheless, there were contaminants left in the carrier gas at levels which will affect the nucleation process.

4 Discussion and conclusions

A saturator was used to produce sulfuric-acid vapor from neat-liquid sulfuric acid for laboratory studies. It was tested and shown to produce similar apparent formation rates during similar conditions to our previous vapor-production method of the furnace. The sulfuric-acid or total-sulfate concentration was measured with two independent methods, and it was shown to produce exact concentrations as prediction from Richardson et al. (1986) and slightly higher than the prediction from Kulmala and Laaksonen (1990) when measured with MARGA (Fig. 3). Concentrations of sulfuric-acid monomer measured with CIMS and CI-Api-TOF was 1–2 orders-of-magnitude lower than the total-sulfate values measured with MARGA and the prediction by Eqs. (1) and (2). The only source of sulfuric acid (sulfate measured by MARGA) is the liquid sulfuric acid inside the saturator as seen in Fig. 3. A possible reason for the discrepancy is that the sulfuric acid is in particle phase since the saturator is a substantial source of particles. However, these particles are lost on the way from the saturator to the nucleation chamber due to two main reasons: (i) the flow rate (0.5 Lpm) in the tube (length: 1 m, I.D. 4 mm) from the saturator to the nucleation chamber is relatively low increasing diffusional losses and (ii) the highly turbulent mixing of the saturator flow with the mixing flow ($Q_{sat} : Q_{mix} \approx 1:30$ or more) transforms the mixer into an effective trap for the particles. The loss of the particles is confirmed with DMPS measurements which cannot explain the discrepancy (Supplement, Fig. S1). Maximum losses to the particle phase in the flow tube are 0–1.4 % with an average below 1 % of the total sulfate. The discrepancy cannot be explained by the formation of larger clusters containing solely sulfuric acid (dimer, trimer, etc.) either, because the concentration of these clusters is of the order of a few percent or lower than the monomer concentration (Supplement, Fig. S5).

The characteristics of the freshly nucleated particles together with the conditions used for the nucleation has been identified and presented (Fig. 4–7). Total losses of sulfuric acid or total sulfate to the whole flow-tube setup have been determined for both methods to detect the concentration of sulfuric acid or total sulfate.

The average total loss factors determined are TLF $= 10.0 \pm 1.2$ ($T_{sat} = 284$–297 K) for MARGA and TLF $= 14.2 \pm 4.2$ ($T_{sat} = 286$–300 K) for CIMS both having a slight increasing deviation from the first-order losses as a function of saturator temperature (Fig. 4). The second-order losses are caused by losses to the particles and losses to the clusters which are too small to be detected by particle counters.

Formation rates of H_2SO_4–H_2O system were compared to our previous studies (Brus et al., 2010, 2011), where a method of the furnace was used (Figs. 8–10). Obtained apparent formation rates as a function of sulfuric-acid or total-sulfate concentrations were independent of the sulfuric-acid vapor-production method (furnace vs. saturator). Conditions for these studies were similar ($T = 298$ K, RH ~ 30 %), but at similar formation rates, the sulfuric-acid monomer concentration is 1–2 orders-of-magnitude lower than the total sulfate. The slope of the fit to the formation-rate data as a function of sulfuric-acid monomer concentration (1.3 ± 0.2) is very similar to that obtained in Brus et al. (2011) (1.2 ± 0.1). The comparison to our previous measurements was done to check reproducibility of the nucleation-experiment results between the sulfuric-acid vapor-production methods and to eliminate the production method as a possible reason for the discrepancy. The discussion and interpretation of the slopes (Sect. 3.1) and comparison to the atmospheric data (Sect. 3.5) can be found in Brus et al. (2011).

Average ammonia concentration of 60 pptv was found in the system for dry conditions and 126 pptv for RH 30 % as a contaminant, and it was independent of the saturator temperature. It is assumed to originate from the purified, dry, particle-free air used as carrier gas and from the ultrapure water used for humidifying the mixing flow. Ammonia concentration is enough to affect the nucleation process itself substantially, but the magnitude of this effect was not studied in this work. Ammonia can bind sulfuric acid by forming clusters, which might reduce the monomer concentration measured with CIMS and CI-Api-TOF slightly. Since the contaminant level was constant and saturator temperature was increased, reducing the contaminant to total sulfate-ratio from $\sim 1:1$ to $\sim 1:10$ for dry conditions and from $\sim 3:1$ to $\sim 1:5$ for humid conditions, it does not explain the discrepancy between the two sulfuric-acid or total-sulfate-detection methods. Even though the contaminant levels might appear high to some, those are still below the most-pure commercially available gases (AGA, N_2, 6.0).

Another possible reason for the difference between sulfuric acid monomer and total sulfate is that sulfuric-acid molecules are most probably bonded to some molecule(s) (e.g. amines, ammonia, organics) and not detected by CIMS or identified from the CI-Api-TOF spectra (Kulmala et al., 2013). As Kurten et al. (2011) state, base molecules can be only in minor importance due to the fact that nitrate ion (NO_3^-) will most probably substitute the base out in the CIMS charging process. Nevertheless, there is expected to be a substantial pool of clusters formed of sulfuric acid-base molecules in our system, which are too small to be detected by current state-of-art particle counters such as PSM. These clusters are the main reason for the discrepancy between measured total-sulfate and the monomer concentrations. Identical or similar clusters are most probably forming in all laboratory nucleation experiments involving sul-

furic acid, as there are always contaminants present in carrier gases. Further analysis of the CI-Api-TOF mass spectra showed a large number of stick-unit masses correlating with sulfuric-acid monomer ion (HSO_4^-), suggesting a large number of clusters containing sulfuric acid which are not used for calculating the sulfuric-acid concentration measured by mass spectrometers (see Supplement, Sect. 6 and Figs. S6–S11). Sulfuric acid (measured here as sulfate) can contribute to the early growth of ultrafine particles to a much larger extent than currently thought, since most of the sulfuric acid remains undetected. Also the huge number of correlating masses with increasing sulfuric-acid concentration implies that there are numerous substances that can form stable clusters with sulfuric acid that may be the starting point for particle formation.

The total sulfate (originally total sulfuric acid) is responsible for the particle growth as demonstrated in Skrabalova et al. (2014). The contribution of the total sulfate to the nucleation process itself is not yet fully understood. However, recent results suggest that sulfuric-acid monomer concentration is the main component in nucleation (Brus et al., 2015) and not the overall sulfuric acid. To find out which molecules are possibly involved in nucleation, the clusters with sulfuric acid must be identified from the CI-Api-TOF spectra.

The Supplement related to this article is available online at doi:10.5194/acp-15-3429-2015-supplement.

Acknowledgements. The financial support by the Academy of Finland Centre of Excellence program (project no. 1118615), KONE foundation and by the Maj and Tor Nessling Foundation are gratefully acknowledged. The language improvements provided by Curtis Wood are gratefully acknowledged.

Edited by: A. Virtanen

References

Arnold, F.: Ion-induced nucleation of atmospheric water vapor at the mesopause, Planet. Space Sci., 28, 1003–1009, doi:10.1016/0032-0633(80)90061-6, 1980.

Ayers, G. P., Gillett, R. W., and Gras, J. L.: On the vapor pressure of sulphuric acid, Geophys. Res. Lett., 7, 433–436, 1980.

Ball, S. M., Hanson, D. R., and Eisele, F. L.: Laboratory studies of particle nucleation: Initial results for H_2SO_4, H_2O, and NH_3 vapors, J. Geophys. Res., 104, 23709–23718, doi:10.1029/1999JD900411, 1999.

Benson, D., Young, L.-H., Kameel, F., and Lee, S.-H.: Laboratory-measured nucleation rates of sulfuric acid and water binary homogeneous nucleation from the SO_2+ OH reaction, Geophys. Res. Lett., 35, L11801, doi:10.1029/2008GL033387, 2008.

Benson, D. R., Erupe, M. E., and Lee, S.-H.: Laboratory-measured H_2SO_4-H_2O-NH_3 ternary homogeneous nucleation rates: Initial observations, Geophys. Res. Lett., 36, L15818, doi:10.1029/2009GL038728, 2009.

Benson, D. R., Yu, J. H., Markovich, A., and Lee, S.-H.: Ternary homogeneous nucleation of H_2SO_4, NH_3, and H_2O under conditions relevant to the lower troposphere, Atmos. Chem. Phys., 11, 4755–4766, doi:10.5194/acp-11-4755-2011, 2011.

Berndt, T., Stratmann, F., Bräsel, S., Heintzenberg, J., Laaksonen, A., and Kulmala, M.: SO_2 oxidation products other than H_2SO_4 as a trigger of new particle formation. Part 1: Laboratory investigations, Atmos. Chem. Phys., 8, 6365–6374, doi:10.5194/acp-8-6365-2008, 2008.

Berndt, T., Stratmann, F., Sipilä, M., Vanhanen, J., Petäjä, T., Mikkilä, J., Grüner, A., Spindler, G., Lee Mauldin III, R., Curtius, J., Kulmala, M., and Heintzenberg, J.: Laboratory study on new particle formation from the reaction OH + SO_2: influence of experimental conditions, H_2O vapour, NH_3 and the amine tert-butylamine on the overall process, Atmos. Chem. Phys., 10, 7101–7116, doi:10.5194/acp-10-7101-2010, 2010.

Berresheim, H., Elste, T., Plass-Dülmer, C. Eisele, F. L., and Tanner, D. J.: Chemical ionization mass spectrometer for long-term measurements of atmospheric OH and H_2SO_4, Int. J. Mass Spectrom., 202, 91–109, 2000.

Brus, D., Hyvärinen, A.-P., Viisanen, Y., Kulmala, M., and Lihavainen, H.: Homogeneous nucleation of sulfuric acid and water mixture: experimental setup and first results, Atmos. Chem. Phys., 10, 2631–2641, doi:10.5194/acp-10-2631-2010, 2010.

Brus, D., Neitola, K., Hyvärinen, A.-P., Petäjä, T., Vanhanen, J., Sipilä, M., Paasonen, P., Kulmala, M., and Lihavainen, H.: Homogenous nucleation of sulfuric acid and water at close to atmospherically relevant conditions, Atmos. Chem. Phys., 11, 5277–5287, doi:10.5194/acp-11-5277-2011, 2011.

Brus, D., Hyvärinen, A.-P., Anttila, T., Neitola, K., Koskinen, J., Makkonen, U., Hellén, H., Hemmilä, M., Sipilä, M., Mauldin III, R. L., Jokinen, T., Petäjä, T., Kurtén, T., Vehkamäki, H., Kulmala, M., Viisanen, Y., Lihavainen, H., and Laaksonen, A.: Reconsidering the sulphuric acid saturation vapour pressure: Classical Nucleation Theory revived, Phys. Rev. Lett., in review, 2015.

Davidson, C., Phalen, R., and Solomon P.: Airborne Particulate Matter and Human Health: a Review, Aerosol Sci. Tech., 39, 737–749, doi:10.1080/02786820500191348, 2005.

Eisele, F. and Tanner, D.: Measurement of the gas phase concentration of H_2SO_4 and methane sulfonic acid and estimates of H_2SO_4 production and loss in the atmosphere, J. Geophys. Res., 98, 9001–9010, doi:10.1029/93JD00031, 1993.

Feingold, G. and Siebert, H.: Chapter 14 Cloud-Aerosol Interactions from the Micro to the Cloud Scale, in Clouds in the Perturbed Climate System, edited by: Heintzenberg, J. and Charlson, R. J., 319–338, The MIT Press, Cambridge, 2009.

Herrmann, E., Brus, D., Hyvärinen, A.-P., Stratmann, F., Wilck, M., Lihavainen, H., and Kulmala, M.: A computational fluid dynamics approach to nucleation in the water-sulfuric acid system, J. Phys. Chem. A, 114, 8033–8042, 2010.

Hirsikko, A., Nieminen, T., Gagné, S., Lehtipalo, K., Manninen, H. E., Ehn, M., Hõrrak, U., Kerminen, V.-M., Laakso, L., McMurry, P. H., Mirme, A., Mirme, S., Petäjä, T., Tammet, H., Vakkari, V., Vana, M., and Kulmala, M.: Atmospheric ions and nucleation: a review of observations, Atmos. Chem. Phys., 11, 767–798, doi:10.5194/acp-11-767-2011, 2011.

Jokinen, V. and Mäkelä, J. M.: Closed-loop arrangement with critical orifice for DMA sheath/ excess flow system, J. Aerosol Sci., 28, 643–648, 1997.

Jokinen, T., Sipilä, M., Junninen, H., Ehn, M., Lönn, G., Hakala, J., Petäjä, T., Mauldin III, R. L., Kulmala, M., and Worsnop, D. R.: Atmospheric sulphuric acid and neutral cluster measurements using CI-APi-TOF, Atmos. Chem. Phys., 12, 4117–4125, doi:10.5194/acp-12-4117-2012, 2012.

Junninen, H., Ehn, M., Petäjä, T., Luosujärvi, L., Kotiaho, T., Kostiainen, R., Rohner, U., Gonin, M., Fuhrer, K., Kulmala, M., and Worsnop, D. R.: A high-resolution mass spectrometer to measure atmospheric ion composition, Atmos. Meas. Tech., 3, 1039–1053, doi:10.5194/amt-3-1039-2010, 2010.

Kerminen, V.-M., Petäjä, T., Manninen, H. E., Paasonen, P., Nieminen, T., Sipilä, M., Junninen, H., Ehn, M., Gagné, S., Laakso, L., Riipinen, I., Vehkamäki, H., Kurten, T., Ortega, I. K., Dal Maso, M., Brus, D., Hyvärinen, A., Lihavainen, H., Leppä, J., Lehtinen, K. E. J., Mirme, A., Mirme, S., Hõrrak, U., Berndt, T., Stratmann, F., Birmili, W., Wiedensohler, A., Metzger, A., Dommen, J., Baltensperger, U., Kiendler-Scharr, A., Mentel, T. F., Wildt, J., Winkler, P. M., Wagner, P. E., Petzold, A., Minikin, A., Plass-Dülmer, C., Pöschl, U., Laaksonen, A., and Kulmala, M.: Atmospheric nucleation: highlights of the EUCAARI project and future directions, Atmos. Chem. Phys., 10, 10829–10848, doi:10.5194/acp-10-10829-2010, 2010.

Kirkby, J., Curtius, J., Almeida, J., Dunne, E., Duplissy, J., Ehrhart, S., Franchin, A., Gagné, S., Ickes, L., Kürten, A., Kupc, A., Metzger, A., Riccobono, F., Rondo, L., Schobesberger, S., Tsagkogeorgas, G., Wimmer, D., Amorim, A., Bianchi, F., Breitenlechner, M., David, A., Dommen, J., Downard, A., Ehn, M., Flagan, R., Haider, S., Hansel, A., Hauser, D., Jud, W., Junninen, H., Kreissl, F., Kvashin, A., Laaksonen, A., Lehtipalo, K., Lima, J., Lovejoy, E., Makhmutov, V., Mathot, S., Mikkilä, J., Minginette, P., Mogo, S., Nieminen, T., Onnela, A., Pereira, P., Petäjä, T., Schnitzhofer, R., Seinfeld, J., Sipilä, M., Stozhkov, Y., Stratmann, F., Tomé, A., Vanhanen, J., Viisanen, Y., Aron Vrtala, A., Wagner, P., Walther, H., Weingartner, E., Wex, H., Winkler, P., Carslaw, K., Worsnop, D., Baltensperger, U., and Kulmala, M.: Role of sulphuric acid, ammonia and galactic cosmic rays in atmospheric aerosol nucleation, Nature, 476, 429–433, doi:10.1038/nature10343, 2011.

Korhonen, P., Kulmala, M., Laaksonen, A., Viisanen, Y., McGraw, R., and Seinfeld, J. H.: Ternary nucleation of H_2SO_4, NH_3 and H_2O in the atmosphere, J. Geophys. Res., 104, 26349–26353, doi:10.1029/1999JD900784, 1999.

Kulmala, M. and Laaksonen, A.: Binary nucleation of water-sulfuric acid system: Comparison of classical theories with different H_2S0_4 saturation vapor pressures, J. Chem. Phys., 93, 696, doi:10.1063/1.459519, 1990.

Kulmala, M., Vehkamäki, H., Petäjä, T., Dal Mas,o M., Lauri, A., Kerminen, V.-M., Birmili, W., and McMurry, P. H.: Formation and growth rates of ultrafine atmospheric particles: A review of observations, J. Aerosol Sci., 35, 143–176, doi:10.1016/j.jaerosci.2003.10.003, 2004.

Kulmala, M., Lehtinen, K. E. J., and Laaksonen, A.: Cluster activation theory as an explanation of the linear dependence between formation rate of 3nm particles and sulphuric acid concentration, Atmos. Chem. Phys., 6, 787–793, doi:10.5194/acp-6-787-2006, 2006.

Kulmala, M., Riipinen, I., Sipilä, M., Manninen, H. E., Petäjä, T., Junninen, H., Dal Maso, M., Mordas, G., Mirme, A., Vana, M., Hirsikko, A., Laakso, L., Harrison, R. M., Hanson, I., Leung, C., Lehtinen, K. E. J., and Kerminen, V.-M.: Towards direct measurement of atmospheric nucleation, Science, 318, 89–92, doi:10.1126/science.1144124, 2007.

Kulmala, M., Petäjä, T., Nieminen, T., Sipilä, M., Manninen, H. E., Lehtipalo, K., Dal Maso, M., Aalto, P. P., Junninen, H., Paasonen, P., Riipinen, I., Lehtinen, K. E. J., Laaksonen, K. E. J., and Kerminen, V.-M.: Measurement of the nucleation of atmospheric aerosol particles, Nature Protoc., 7, 1651–1667, doi:10.1038/nprot.2012.091, 2012.

Kulmala, M., Kontkanen, J., Junninen, H., Lehtipalo, K., Manninen, H. E., Nieminen, T., Petäjä, T., Sipilä, M., Schobesberger, S., Rantala, P., Franchin, A., Jokinen, T., Järvinen, E., Äijälä, M., Kangasluoma, J., Hakala, J., Aalto, P. P., Paasonen, P., Mikkilä, J., Vanhanen, J., Aalto, J., Hakola, H., Makkonen, U., Ruuskanen, T., Mauldin III, R. L., Duplissy, J., Vehkamäki, H., Bäck, J., Kortelainen, A., Riipinen, I., Kurten, T., Johnston, M. V., Smith, J. N., Ehn, M., Mentel, T. F., Lehtinen, K. E. J., Laaksonen, A., Kerminen, V.-M., and Worsnop, D. R.: Direct observations of atmospheric aerosol nucleation, Science, 339, 943–946, 2013.

Kurtén, T., Petäjä, T., Smith, J., Ortega, I. K., Sipilä, M., Junninen, H., Ehn, M., Vehkamäki, H., Mauldin, L., Worsnop, D. R., and Kulmala, M.: The effect of H_2SO_4 – amine clustering on chemical ionization mass spectrometry (CIMS) measurements of gas-phase sulfuric acid, Atmos. Chem. Phys., 11, 3007–3019, doi10.5194/acp-11-3007-2011, 2011.

Kürten, A., Rondo, L., Ehrhart, S., and Curtius, J.: Calibration of a Chemical Ionization Mass Spectrometer for the Measurement of Gaseous Sulfuric Acid, J. Phys. Chem. A, 116, 6375–6386, 2012.

Lee, S.-H., Reeves, J. M., Wilson, J. C., Hunton, D. E., Viggiano, A. A.,Miller, T. M., Ballenthin, J. O., and Lait, L. R.: Particle Formation by Ion Nucleation in the Upper Troposphere and Lower Stratosphere, Science, 301, 1886–1889, doi:10.1126/science.1087236, 2003.

Lihavainen, H., Kerminen, V.-M., Komppula, M., Hatakka, J., Aaltonen, V., Kulmala, M., and Viisanen Y.: Production of "potential" cloud condensation nuclei associated with atmospheric new-particle formation in northern Finland, J. Geophys. Res., 108, 4782, doi:10.1029/2003JD003887, 2003.

Lihavainen, H., Kerminen, V.-M., Tunved, P., Aaltonen, V., Arola, A., Hatakka, J., Hyvärinen, A. and Viisanen, Y.: Observational signature of the direct radiative effect by natural boreal forest aerosols and its relation to the corresponding first indirect effect, J. Geophys. Res. 114, 2156–2202, doi:10.1029/2009JD012078, 2009.

Lovejoy, E. R., Curtius, J., and Froyd, K. D.: Atmospheric ion-induced nucleation of sulphuric acid and water, J. Geophys. Res., 109, D08204, doi:10.1029/2003JD004460, 2004.

Makkonen, U., Virkkula, A., Mäntykenttä, J., Hakola, H., Keronen, P., Vakkari, V., and Aalto, P. P.: Semi-continuous gas and inorganic aerosol measurements at a Finnish urban site: comparisons with filters, nitrogen in aerosol and gas phases, and aerosol acidity, Atmos. Chem. Phys., 12, 5617–5631, doi:10.5194/acp-12-5617-2012, 2012.

Manninen, H. E., Nieminen, T., Asmi, E., Gagné, S., Häkkinen, S., Lehtipalo, K., Aalto, P., Vana, M., Mirme, A., Mirme, S.,

Hõrrak, U., Plass-Dülmer, C., Stange, G., Kiss, G., Hoffer, A., Töro, N., Moerman, M., Henzing, B., de Leeuw, G., Brinkenberg, M., Kouvarakis, G. N., Bougiatioti, A., Mihalopoulos, N., O'Dowd, C., Ceburnis, D., Arneth, A., Svenningsson, B., Swietlicki, E., Tarozzi, L., Decesari, S., Facchini, M. C., Birmili, W., Sonntag, A., Wiedensohler, A., Boulon, J., Sellegri, K., Laj, P., Gysel, M., Bukowiecki, N., Weingartner, E., Wehrle, G., Laaksonen, A., Hamed, A., Joutsensaari, J., Petäjä, T., Kerminen, V.-M., and Kulmala, M.: EUCAARI ion spectrometer measurements at 12 European sites – analysis of new particle formation events, Atmos. Chem. Phys., 10, 7907–7927, doi:10.5194/acp-10-7907-2010, 2010.

Mauldin III, R. L., Frost, G., Chen, G., Tanner, D., Prevot, A., Davis, D., and Eisele, F.: OH measurements during the First Aerosol Characterization Experiment (ACE 1): Observations and model comparisons, J. Geophys. Res., 103, 16713–16729, doi:10.1029/98JD00882, 1998.

Merikanto, J., Spracklen, D. V., Mann, G. W., Pickering, S. J., and Carslaw, K. S.: Impact of nucleation on global CCN, Atmos. Chem. Phys., 9, 8601–8616, doi:10.5194/acp-9-8601-2009, 2009.

Napari, I., Noppel, M., Vehkamäki, H., and Kulmala M.: Parametrization of ternary nucleation rates for H_2SO_4-NH_3-H_2O vapors, J. Geophys. Res., 107, 4381, doi:10.1029/2002JD002132, 2002.

Nieminen, T., Paasonen, P., Manninen, H. E., Sellegri, K., Kerminen, V.-M., and Kulmala, M.: Parameterization of ion-induced nucleation rates based on ambient observations, Atmos. Chem. Phys., 11, 3393–3402, doi:10.5194/acp-11-3393-2011, 2011.

Paasonen, P., Nieminen, T., Asmi, E., Manninen, H. E., Petäjä, T., Plass-Dülmer, C., Flentje, H., Birmili, W., Wiedensohler, A., Hõrrak, U., Metzger, A., Hamed, A., Laaksonen, A., Facchini, M. C., Kerminen, V.-M., and Kulmala, M.: On the roles of sulphuric acid and low-volatility organic vapours in the initial steps of atmospheric new particle formation, Atmos. Chem. Phys., 10, 11223–11242, doi:10.5194/acp-10-11223-2010, 2010.

Petäjä, T., Mauldin, III, R. L., Kosciuch, E., McGrath, J., Nieminen, T., Paasonen, P., Boy, M., Adamov, A., Kotiaho, T., and Kulmala, M.: Sulfuric acid and OH concentrations in a boreal forest site, Atmos. Chem. Phys., 9, 7435–7448, doi:10.5194/acp-9-7435-2009, 2009.

Richardson, C. B., Hightower, R. L., and Pigg, A. L.: Optical measurements of evaporation of sulphuric acid droplets, Appl. Optics, 25, 1226–1229, 1986.

Sipilä, M., Berndt, T., Petäjä, T., Brus, D., Vanhanen, J., Stratmann, F., Patokoski, J., Mauldin III, Roy, L., Hyvärinen, A.-P., Lihavainen, H., and Kulmala, M.: The role of sulphuric acid in atmospheric nucleation, Science, 327, 1243–1246, doi:10.1126/science.1180315, 2010.

Skrabalova, L., Brus, D., Anttila, T., Zdimal, V., and Lihavainen, H.: Growth of sulphuric acid nanoparticles under wet and dry conditions, Atmos. Chem. Phys., 14, 6461–6475, doi:10.5194/acp-14-6461-2014, 2014.

Slanina, J., ten Brink, H. M., Otjes, R. P., Even, A., Jongejan, P., Khlystov, S., Waijers-Ijpelaan, A., Hu, M., and Lu, Y.: The continuous analysis of nitrate and ammonium in aerosols by the steam jet aerosol collector (SJAC): extension and validation of the methodology, Atmos. Environ., 35, 2319–2330, doi:10.1016/S1352-2310(00)00556-2, 2001.

Spracklen, D. V., Carslaw, K. S., Kulmala, M., Kerminen, V.-M., Mann, G. W., and Sihto, S.-L.: The contribution of boundary layer nucleation events to total particle concentrations on regional and global scales, Atmos. Chem. Phys., 6, 5631–5648, doi:10.5194/acp-6-5631-2006, 2006.

ten Brink, H., Otjes, R., Jongejan, P., and Slanina S.: An instrument for semi-continuous monitoring of the size-distribution of nitrate, ammonium, sulphate and chloride in aerosol, Atmos. Environ., 41, 2768–2779, doi:10.1016/j.atmosenv.2006.11.041, 2007.

Vanhanen, J., Mikkilä, J., Lehtipalo, K., M. Sipilä, M., Manninen, H., Siivola, E., Petäjä, T., and Kulmala, M.: Aerosol Sci. Tech., 45, 533–542, doi:10.1080/02786826.2010.547889, 2011.

Vehkamäki, H., Kulmala, M., Napari, I., Lehtinen, K. E. J., Timmreck, C., Noppel, M., and Laaksonen A.: An improved parameterization for sulfuric acid-water nucleation rates for tropospheric and stratospheric conditions, J. Geophys. Res., 107, 4622, doi:10.1029/2002JD002184, 2002.

Viisanen, Y., Kulmala, M., and Laaksonen, A.: Experiments on gas-liquid nucleation of sulfuric acid and water, J. Chem. Phys., 107, 920–926, doi:10.1063/1.474445, 1997.

Weber, R. J., Marti, J. J., McMurry, P. H., Eisele, F. L., Tanner, D. J., and Jefferson, A.: Measured atmospheric new particle formation rates: Implications for nucleation mechanisms, Chem. Eng. Commun., 151, 53–64, doi:10.1080/00986449608936541, 1996.

Wiedensohler, A. and Fissan, H. J.: Bipolar Charge Distributions of Aerosol Particles in High-Purity Argon and Nitrogen, Aerosol Sci. Tech., 14, 358–364, doi:10.1080/02786829108959498, 1991.

Winkler, P. M., Steiner, G., Vrtala, A., Vehkamäki, H., Noppel, M., Lehtinen, K. E. J., Reischl, G. P., Wagner, P. E., and Kulmala, M.: Heterogeneous Nucleation Experiments Bridging the Scale from Molecular Ion Clusters to Nanoparticles, Science, 319, 1374–1377, doi:10.1126/science.1149034, 2008.

Wyslouzil, B. E., Seinfeld, J. H., and Flagan, R. C.: Binary nucleation in acid-water systems. I. Methanesulfonic acid-water, J. Chem. Phys., 94, 6842, doi:10.1063/1.460261, 1991.

Young, L. H., Benson, D. R., Kameel, F. R., Pierce, J. R., Junninen, H., Kulmala, M., and Lee, S.-H.: Laboratory studies of H_2SO_4/H_2O binary homogeneous nucleation from the $SO_2 + OH$ reaction: evaluation of the experimental setup and preliminary results, Atmos. Chem. Phys., 8, 4997–5016, doi:10.5194/acp-8-4997-2008, 2008.

Yu, F.: From molecular clusters to nanoparticles: second-generation ion-mediated nucleation model, Atmos. Chem. Phys., 6, 5193–5211, doi:10.5194/acp-6-5193-2006, 2006.

Yu, F., Wang, Z., Luo, G., and Turco, R.: Ion-mediated nucleation as an important global source of tropospheric aerosols, Atmos. Chem. Phys., 8, 2537–2554, doi:10.5194/acp-8-2537-2008, 2008.

Yu, F.: Ion-mediated nucleation in the atmosphere: Key controlling parameters, implications, and look-up table, J.Geophys. Res., 115, D03206, doi:10.1029/2009JD012630, 2010.

Zhang, R., Khalizov, A. F., Wang, L., Hu, M., and Xu, W.: Nucleation and growth of nanoparticles in the atmosphere, Chem. Rev., 112, 1957–2011, doi:10.1021/cr2001756, 2012.

Zheng, J., Khalizov, A., Wang, L., and Zhang, R.: Atmospheric Pressure-Ion Drift Chemical Ionization Mass Spectrometry for Detection of Trace Gas Species, Anal. Chem., 82, 7302–7308, doi:10.1021/ac101253n, 2010.

Zollner, J. H., Glasoe, W. A., Panta, B., Carlson, K. K., McMurry, P. H., and Hanson, D. R.: Sulfuric acid nucleation: power dependencies, variation with relative humidity, and effect of bases, Atmos. Chem. Phys., 12, 4399–4411, doi:10.5194/acp-12-4399-2012, 2012.